CDC
Workplace Safety and Health

RI 9662

REPORT OF INVESTIGATIONS/2004

Evaluation of Instrumented Cable Bolts in Cement Grout to Determine Physical and Numerical Modeling Properties

Department of Health and Human Services
Centers for Disease Control and Prevention
National Institute for Occupational Safety and Health

NIOSH

Report of Investigations 9662

Evaluation of Instrumented Cable Bolts in Cement Grout to Determine Physical and Numerical Modeling Properties

By Lewis Martin, Doug Milne, Marc Ruest, and Rimas Pakalnis

U.S. DEPARTMENT OF HEALTH AND HUMAN SERVICES
Centers for Disease Control and Prevention
National Institute for Occupational Safety and Health
Spokane Research Laboratory
Spokane, WA

April 2004

ORDERING INFORMATION

Copies of National Institute for Occupational Safety and Health (NIOSH) documents and information about occupational safety and health are available from

NIOSH–Publications Dissemination
4676 Columbia Parkway
Cincinnati, OH 45226-1998

FAX: 513-533-8573
Telephone: 1-800-35-NIOSH
(1-800-356-4674)
E-mail: pubstaft@cdc.gov
Web site: www.cdc.gov/niosh

DHHS (NIOSH) Publication No. 2004-140

CONTENTS

ILLUSTRATIONS

TABLES

UNIT OF MEASURE ABBREVIATIONS USED IN THIS REPORT

cm	centimeter	m•m	meter per meter
GPa	gigapascal	mm	millimeter
kN	kilonewton	MPa	megapascal
kN/m	kilonewton per meter	N	newton
kN/min	kilonewton per minute	N/cm	newton per centimeter
m	meter	∈	microstrain

EVALUATION OF INSTRUMENTED CABLE BOLTS IN CEMENT GROUT TO DETERMINE PHYSICAL AND NUMERICAL MODELING PROPERTIES

By Lewis Martin,[1] Doug Milne,[2] Marc Ruest,[3] and Rimas Pakalnis[4]

ABSTRACT

Whereas many researchers and mine engineers have conducted tests on cable bolts using various grouts, water:cement ratios, and physical modifications of the cable to determine the load-carrying characteristics of a bolt, few studies have been conducted on cable bolts fitted with internal instruments. Those studies that have been done have concentrated on cable response averaged over significant (6.1 m) cable lengths. Researchers at the Spokane Research Laboratory (SRL) of the National Institute for Occupational Safety and Health in Spokane, WA, are investigating the physical properties of cable bolts by replacing the conventional king wire with a modified king wire on which strain gauges have been installed.

A numerical analysis was performed to match laboratory results. Loads calculated by the model were then compared to loads measured in the laboratory on 1.83-m-long cables grouted into two 0.91-m-long pull-tube assemblies. Load along the cable was monitored with 20 strain gauges installed along the length of the cable. This paper documents test results on these modified cable bolts. The instrumented cable bolt provided reproducible point measurements of cable load as opposed to load measurements averaged over long cable lengths. Such point measurements can assist in interpreting the influence of cable confinement, grout quality, rock mass stiffness, and other factors. The instrumented cable bolt is a practical field and research tool because it can predict point loading along the cable.

The instrument has been successfully field tested at FMC's Granger Mine, Granger, WY; the Meikle Mine, Carlin, NV; the Stillwater Mine, Nye, MT; and the Getchell Mine, Golconda, NV. By monitoring load and displacement of the rock mass using these instrumented bolts, more-effective ground support can be selected and installed, which will lead to safer working conditions for miners.

[1]Mechanical engineer, Spokane Research Laboratory, National Institute for Occupational Safety and Health, Spokane, WA.
[2]Mining engineer and associate professor, University of Saskatchewan, Saskatoon, SK.
[3]Mining engineer, Itasca Consulting Group, Inc., Minneapolis, MN.
[4]Mining engineer and professor, University of British Columbia, Vancouver, BC.

INTRODUCTION

Many researchers and mine engineers have conducted a large array of tests to determine the effects of various grouts, water:cement ratios, and physical "enhancements" (Garford bulbs, buttons, birdcage configurations, nut cages, etc.) on the load characteristics of cable bolts (Goris 1990). A limited number of studies have looked at load distribution along a cable bolt. However, tests with instrumented cable bolts installed inside steel pipes have been conducted only with extensometer-type internal instruments (Hyett and Bawden 1997) and externally mounted strain gauges (Chekired et al. 1997; Choquet and Miller 1987; Goris et al. 1993; Windsor and Worotniki 1986).

Well-tested commercial instruments, such as the Tensmeg and the SMART cable, exist for measuring load on cable bolts. The Tensmeg is a 60-cm-long, externally mounted strain gauge, while in the SMART cable, the king wire has been replaced by an extensometer having internal wires anchored along the cable and attached to potentiometers within the electrical head. The difference in displacement between anchors is used to calculate average strain, which is then related to load via cable stiffness.

Strain is defined as change in length over distance. Therefore, a strain gauge measures the change in length (deformation) along some object of previously fixed length. As this length increases, the sensitivity of the strain gauge decreases. The anchor spacings within a SMART cable are usually no less than 1 m, and load and strain are averaged over this length.

The Spokane Research Laboratory (SRL) of the National Institute for Occupational Safety and Health (NIOSH) has developed a new instrumented cable bolt (figure 1) (patent 6,311,564) in which the original king wire has been replaced with a strip of steel (ribbon cable) to which strain gauges have been attached (figure 2). Because of their low cost and small size, many strain gauges can be installed along the cable to get a better understanding of load distribution.

This cable bolt is 1.8 m long and 15.8 mm in diameter and has an ultimate strength of 258 kN. Twenty strain gauges are positioned at 7.6-cm intervals along two sides of the replacement king wire. The cable is then inserted into two 0.9-m-long sections of thick- walled (8.55 mm) steel pipe (so that 10 gauges are in each pipe section) and grouted with Type I/II portland cement at a water:cement mixing ratio of 0.35:1.

The main advantage of the new instrument is that cable axial elongation can be measured over a short distance, thereby providing an accurate estimate of load over a small (approximately 13 mm) length of cable. That is, as the grout transfers axial load to the cable, the strain gauge on the king wire reads elongation in microstrain. Using Hooke's Law, strain can be converted back to load. The instrument has the potential to provide more information than can be obtained from existing cable load monitoring devices. It also provides valuable insights into cable support behavior.

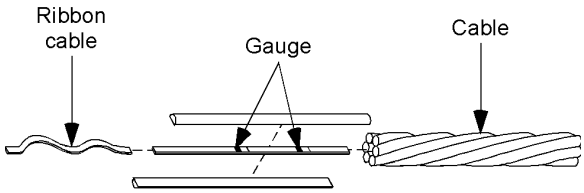

Figure 1.—Instrumented king wire with gauges and connecting cable.

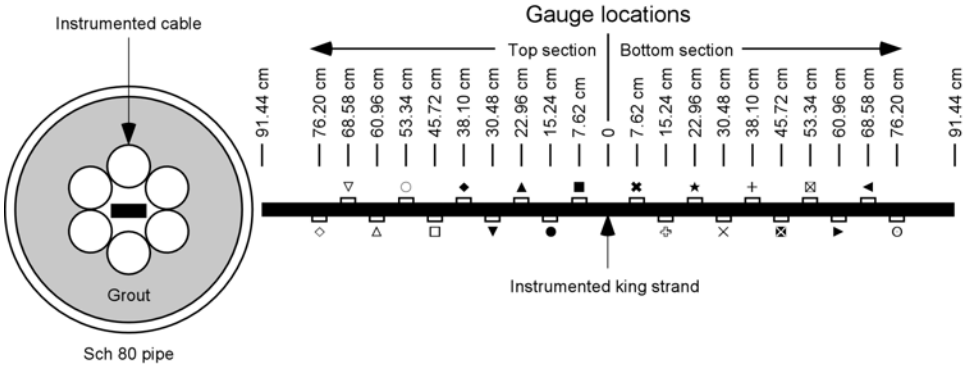

Figure 2.—Instrumented cable grouted in steel pipe.

LABORATORY TESTS

The instrumented SRL cables have a modified geometry and therefore required calibration to determine their behavior. Therefore, pull tests were conducted to compare load to strain along the embedded cable. These tests followed the procedure developed by Goris (1990), and the test apparatus (figure 3) was the same one used by Goris and Conway (1987) during a testing program at the U.S. Bureau of Mines.

Methods of estimating cable load are based on cable stiffness using the equation—

$$P = K \times \epsilon, \quad (1)$$

where P = cable load, kN

K = cable stiffness, kN/(m•m)

and ϵ = cable strain, microstrain.

Manufacturer's specifications state that the common K value is 28,410 kN/(m•m) for a seven-strand cable. Thus calculating P using K is accurate for the elastic deformation range of a cable and is valid up to about 0.8% strain, or 227 kN ($K = P \div \epsilon$).

CALIBRATION TESTS ON UNGROUTED CABLE

To understand the deformation behavior of a grouted cable, it is first necessary to determine the behavior of free (ungrouted) cables.

To conduct these tests, the king wires in five conventional cables were replaced with instrumented king wires to create the new cables. The cables were then loaded to 178 kN of pull, which is the maximum load for elastic cable deformation, to obtain a calibration curve for each gauge (figure 4).

If a cable bolt is deforming, all measured strains on each strand should be the same. Therefore, a simple approach to determining the stiffness of a six-strand instrumented cable is to assume that the king wire carries one-seventh of the cable load, which would give a stiffness of 24,500 kN/(m•m) for a six-strand cable.

The slope of load-versus-microstrain in figure 4 shows the stiffness of the instrumented cable. The instrumented king wire on the SRL instrumented cable did not carry appreciable load. The drift observed was largely due to the length of the lead wire connecting the individual gauges and was taken into account through the use of an average calibration curve (figure 4).

Calibration test 3 indicated an instrumented cable stiffness that ranged between 21,528 and 25,264 kN/(m•m) at an applied load of 178 kN, which brackets the expected stiffness for a standard cable with one strand removed (or six-sevenths of the standard seven-strand stiffness). A range in values of measured stiffness may be due to differential movement between a king wire and the six external cable strands. A second source of variation may be the position of individual strain gauges with respect to the cable strands. That is, higher strain (lower stiffness) may correspond to gauges positioned directly under a cable strand where slip between the instrumented king wire and the cable strands is unlikely.

PULL TESTS ON GROUTED CABLE

A large database of results from pull tests exists for conventional cables grouted in steel pipes with cement grouts. The load-to-deformation behavior of standard seven-strand cables can be obtained from cable manufacturers.

Three “split-pipe” pull tests were conducted on three instrumented cables that had been grouted into steel pipes. These tests were intended to duplicate crack dilation in underground mine environments and to provide a load profile for the bolt (figure 5).

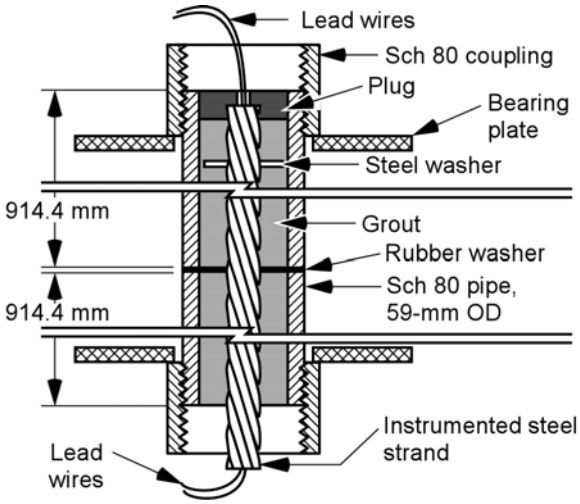

Figure 3.—Pull-test apparatus.

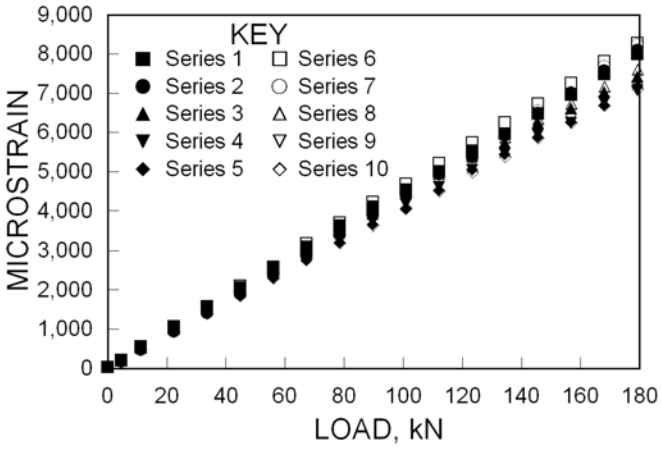

Figure 4.—Calibration curve for instrumented cable bolt.

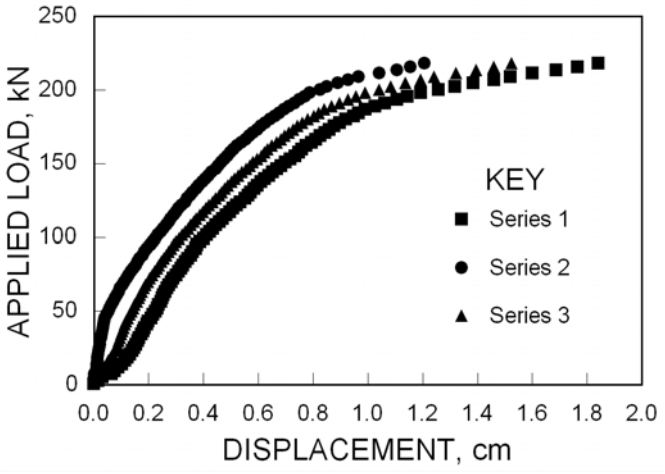

Figure 5.—Displacement pull tests.

Continuous readings of load, strain, and displacement in the cable bolt were taken throughout the test at a load rate of 2.2 kN/min. Load readings were collected electronically from a load cell within the test machine. To verify that the readings from the test apparatus were correct, displacement readings were also obtained from a micrometer attached to the pull tubes and an LVDT on the machine.

At 28 days of grout curing, the first pipe was pulled apart, and the resulting load, displacement, and strain at various points along the cable were measured. An average grout compressive strength of 57 MPa was achieved at 28 days. The second and third tests were conducted after 30 days. The tests were run on all three samples until the cable-grout bond failed. In all three tests, the grout failed before the cable; however, the cables were all undergoing plastic deformation.

Figure 5 shows pull-test results plotted as applied load in kilonewtons versus displacement in centimeters. In each test, the maximum applied load was 200 kN, which is the yield point of the instrumented cable. The plotted displacements are the total displacements measured with LVDT's at the free ends of the cable.

TEST INTERPRETATION: LOAD VERSUS STRAIN FOR GROUTED CABLE

Deformation-based estimates of cable load relate load to deformation by simply dividing deformation by monitored distance to approximate strain and multiplying the result by cable stiffness. This gives an average load or strain along the measured length.

Substantial work has been conducted looking at load distribution along fully grouted bolts (Hyett et al. 1996). In this study, a simplified approach was taken to interpret behavior on the instrumented cable based on observed cable response. The gauges installed 76.2 cm from the load point did not show significant loading until a load of approximately 156 kN had been applied. The gauges at 38.1 cm showed loading at approximately half of 156 kN, or 78 kN. This load transfer rate can be expressed as C, the ratio of loaded cable length to applied load. Therefore, the load at which each strain gauge will start to deform can be estimated as follows:

$$P_o = L_o/C \qquad (2)$$

where P_o = applied load required to initiate deformation of strain gauge, N

L_o = distance of strain gauge from applied load or point of dilation, cm

and C = ratio of cable length-to-applied load.

Thus, $C = 76.2 \text{ cm} / 156 \text{ kN} = 4.89 \times 10^{-1}$ cm/kN.

After a strain gauge on the cable has started to take load, any additional load will increase strain on the gauge directly. Strain will be related to the increase in load based on K (cable stiffness), or ~24,019 kN/(m•m) [six-sevenths of 28,410 kN/(m•m) —the common value for standard seven-strand cable] for the six-strand cables used in this research.

Based on the load transfer rate and cable stiffness, theoretical strain-versus-load curves (figure 6) were calculated for three of the gauges monitored in pull test 2. There was reasonably good agreement between measured and theoretical strains for the gauge at 76.2 cm and excellent agreement for the gauge at 38.1 cm. At high strain values, measured microstrain exceeded theoretical microstrain because the cable had exceeded the 0.8% elastic strain limit. The good agreement for the gauges at 76.2 and 38.1 cm suggests that the basic approach for calculating a constant load transfer rate for instrumented cables is reasonable.

Agreement was not as good between measurements and theory for the gauge at 68.6 cm. It appears that the instrumented king wire was being pulled past the outer cable strands, which would result in low strain readings well before the cable could be expected to carry load. Slip of the instrumented king wire at 68.6 cm would explain the lower-than-expected strain values when the gauge should be loaded (figure 6). This gauge is close to the free end of the cable, and it is possible that untwisting of this end contributed to the lower-than-expected strains at this location.

Additional data from tests at the Noranda Technology Centre (NTC), Montreal, Quebec, in 1992 (Milne et al. 1992) support this interpretation. In these experiments, a pull test was done on a 0.91-m-long grouted cable on which strain gauges had been bonded to the external cable strands at 15.2-cm spacings. The load-versus-microstrain graph had a form similar to the curves from the SRL tests (figure 6), and the load transfer rate was approximately 2.28×10^{-1} cm/kN. A maximum load of only 112 kN was applied to the cable because most of the externally bonded strain gauges and wires had failed at this load. The SRL approach of protecting the gauges and wires in a replacement king strand is a more practical situation.

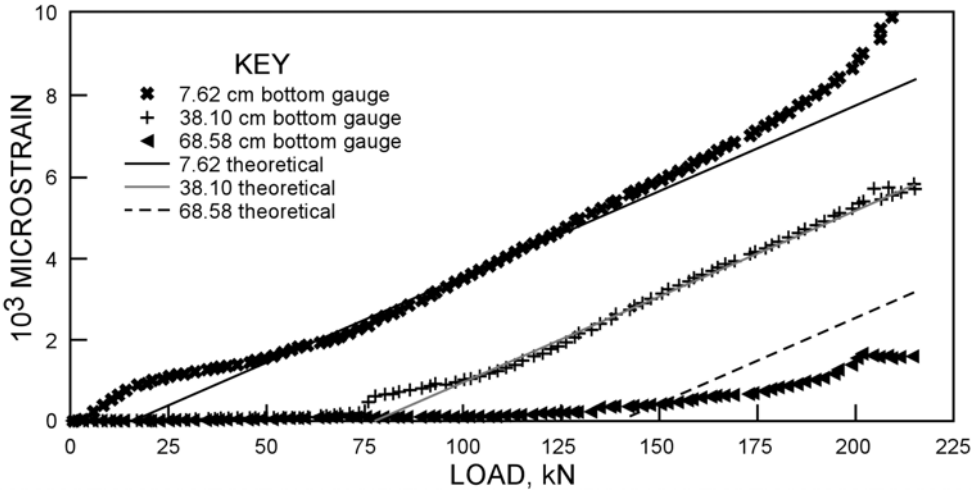

Figure 6.—Graph of measured and calculated strains for three gauges in pull test 2.

COMPARISON OF STANDARD AND NEW SRL CABLE

All approaches for measuring load in cable bolts are based on the principle of measuring deformation over a fixed length and relating the amount to cable stiffness. As the length of the measured distance increases, the accuracy of the estimate of cable strain at a given point may decrease.

It was assumed that load along a grouted cable is driven by dilation of a crack. That is, as a crack expands or lengthens, then cable load increases. Values estimated from SRL tests of six-strand cables are K (on six-strand cables) = 24,019 kN/(m•m) and C (on grouted cables) = 4.89×10^{-1} cm/kN. These values were used in the following analysis. Distances of 91 and 183 cm, which are the typical distances used for monitoring load on conventional cables, were assumed.

Using the load and strain distributions proposed above, load estimates obtained from using various fixed lengths can be compared, as shown in table 1. Table 1 also shows estimates of load at different base lengths for strain gauges installed at various distances from a single dilating crack. A similar qualitative comparison was proposed by Windsor (1992); however, no values were provided. Windsor states that "A discontinuous load profile in a cable is very difficult to measure properly and requires both discrete measurements (i.e., short base length 'cells') and integrated measurements (i.e., long base length 'gauges')."

Table 1 is based on property values used during tests of the SRL instrumented cable. Conventional cables with different grout properties would exhibit different behavior. If several cracks were dilating and loading a grouted cable, much less discrepancy among the different loads would be predicted.

INTERPRETATION OF LOAD PROFILE

Collar load plotted against recorded microstrain at individual gauge locations is shown in figure 7*A*, while load profile along the length of the cable at different collar loads is shown in figure 7*B*. Figure 7*B* also shows the strong correlation between predicted (Eq. 2) and actual loads. When critical load at the collar (x - 0) exceeds 5,204 N × distance of the gauge from the collar (in centimeters), the gauge will commence sensing load so that every incremental change of collar load will equal a similar increase in load on the gauge. This implies that a gauge positioned 25.4 cm from the collar will sense load only when the collar load exceeds 25.4 × 2,043 N/cm, or 51,908 N. When collar load increases from 51,908 to 56,356 N, the gauge at 25.4 cm will sense the incremental load of 4,448 N. Another observation is that the slope of collar load versus microstrain as recorded by the individual gauges parallels the slope of a free cable after a "critical load" has been exceeded (figure 7*A*).

Table 1.–Theoretical load and deformation measured for different cable instruments

Actual cable load, N	Cable length, loaded on each side of crack, cm	Calculated crack dilation, cm	Load based on fixed length, N		Load measured at various distances of SRL gauge from crack, N			
			91 cm	183 cm	0 cm	30.5 cm	45.7 cm	61 cm
22,240	11.2	0.01	2,668	1,334	22,240	0	0	0
44,480	21.8	0.04	10,675	5,337	44,480	0	0	0
88,960	43.7	0.15	42,700	21,350	88,960	222,680	0	0
133,440	65.5	0.36	86,736	48,038	133,440	71,168	40,477	12,899
177,920	87.1	0.64	131,216	84,957	177,920	115,648	84,512	53,376

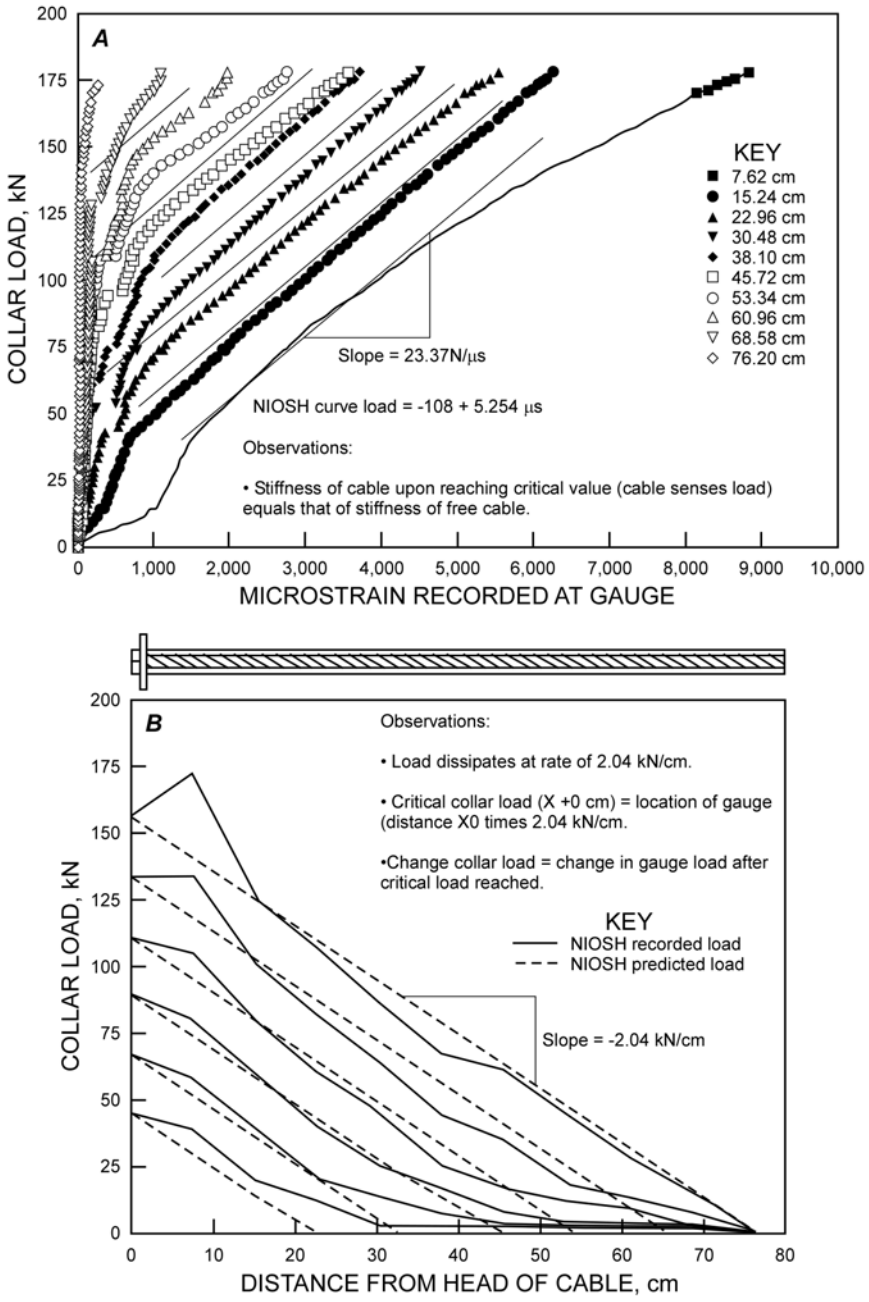

Figure 7.—Collar load plotted against *A*, microstrain (load profile curve) and *B*, distance from head of cable (load correlation curve).

LOAD PROFILE MATRIX

Figure 8*A* shows the critical collar load required before individual gauges on the standard seven-strand cable and the SRL instrumented cable sensed load at various embedment lengths (Goris et al. 1993). The number of wires in contact with the grout is the same for both types of cable. The slopes of the two cables are similar, as would be expected since slope is largely a function of the bond strength of the wire in contact with the grout.

In figure 8*B*, it is assumed that a gauge is positioned every 7.6 cm along the cable. A load of 0 N at the gauge infers a possible load increase of 2.04 kN/cm. Therefore, on the graph, gauges positioned 1.2 m apart indicate a load of 125 kN at point x ~ 76.2 cm, as do the gauges at 15.2 and 137.2 cm. These figures are based on the assumption that there is a single crack. Alternatively, a gauge located at point x ~ 76.2 cm and indicating a load of 0 N negates this possibility. However, an interpreted load of 62 kN is possible if a crack were positioned midway between the gauge at 15.2 cm and the gauge at 76.2 cm.

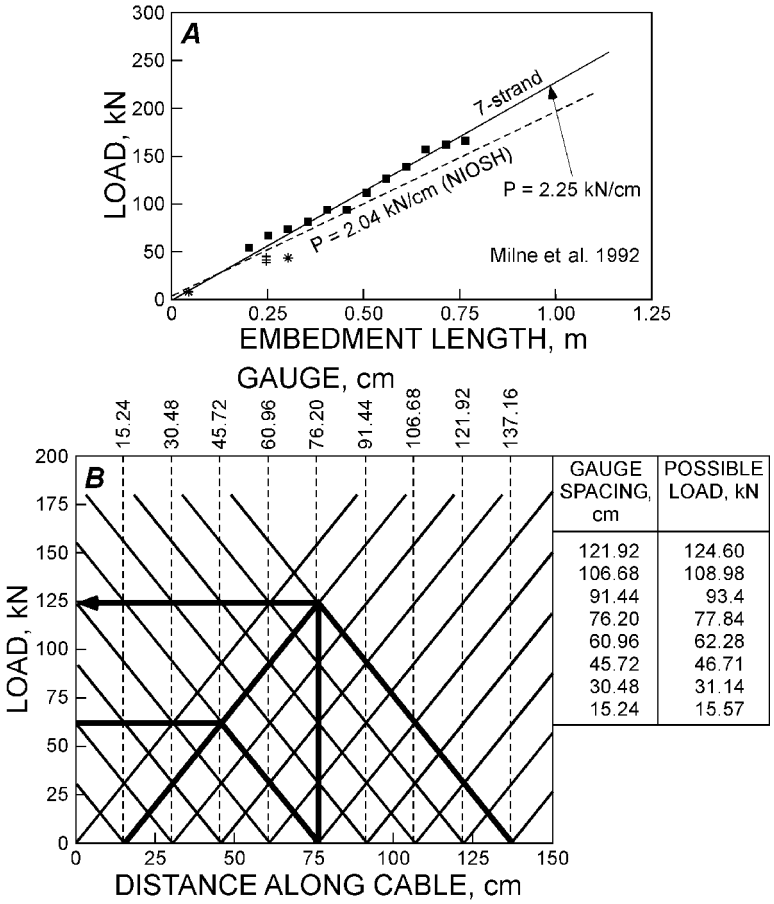

Figure 8.—Load profile matrices. *A*, Load versus embedment length. Squares indicate data points. *B*, Load matrix graph.

This method should be employed when estimating predicted load on a crack using measurements recorded in situ and projecting these measurements to the interpreted location of the crack. This situation is presented in table 1 and shows that it is critical to interpret loading based on measured conditions rather than relying on a single load reading or an average of loads.

SPLIT-PIPE TEST RESULTS FROM FLAC

Strain measured by the strain gauges is related to load on the cable bolt by the stiffness determined from the calibration. The results from the laboratory experiment are provided in terms of measured strain at 7.6-cm intervals along the length of the cable versus applied load to the cable. A plot of applied load-versus-measured microstrain for the first experiment is shown in figure 9.

It is convenient to compare load measured on the instrumented cable and load calculated by Itasca's (2000) computer code Fast Lagrangian Analysis of Continua (FLAC) to determine increments of applied load. For the purpose of this analysis, laboratory-measured and FLAC-calculated loads were compared at 22.2-kN increments. Because the experiment was symmetrical on both sides of the split, it was assumed that the gauges measured identical loads at identical distances away from the split. It was therefore valid to average loads for each of the three tests. In total, six data series for load-versus-applied load were averaged to provide one "idealized" data set to compare with FLAC results (figure 10).

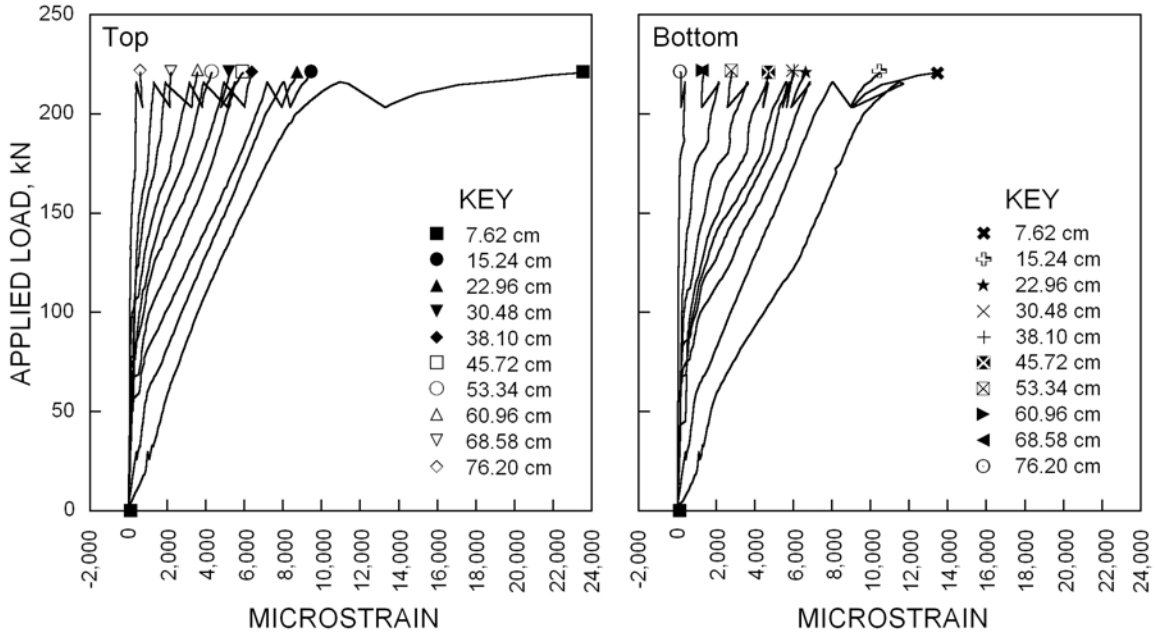

Figure 9.—Pull test 1.

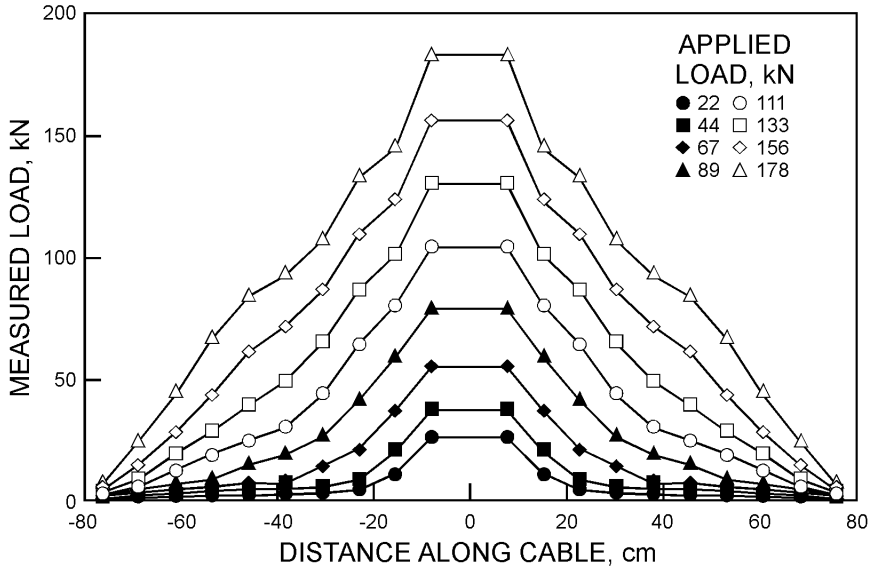

Figure 10.—Idealized measured load versus distance.

MODEL BOUNDARY CONDITIONS AND MATERIAL PROPERTIES

The geometry and boundary conditions for the FLAC model are illustrated in figure 11. In the model, the cable is represented as a series of elements attached at nodes, and the split pipe is represented by two rows of zones. The two rows of zones are "split" at the model's center by detaching the grid points so that both ends of the pipe are free to separate without lateral constraint. The grout bonding the cable to the pipe is implicit in the cable bolt logic. To simulate pulling the split pipe apart, a velocity boundary was applied to both ends of the model. This is analogous to a laboratory test in which each end of the pipe is pulled apart at a constant rate.

The behavior of the FLAC cable element is a function of the behavior of the steel cable (axial behavior) and of the grout-steel cable interface (shear behavior). Because it is slender, the cable

element does not offer any resistance to bending. A simple linear relationship between applied strain and the resulting force describes the axial behavior of the steel. The cable can theoretically take load in either compression or in tension, but in the following analysis, only tensile behavior is relevant.

Figure 12 schematically illustrates cable axial behavior. The required properties for the cable are its tensile strength, Young's modulus, and cross-sectional area (labeled "yield," "E area," and "ycomp," respectively, in the figure). The assumed dimensions and properties for the cable are summarized in table 2. For the purpose of this experiment, yield strength was not relevant because the applied load was kept below the yield strength of the cable.

Shear behavior plays an important role in how a cable is loaded when the grid is displaced. It is through the grout-cable interface that grid displacement induces load in the cable via shear stress. The shear behavior of the grout is represented as a spring-slider system at the cable nodes (figure 13).

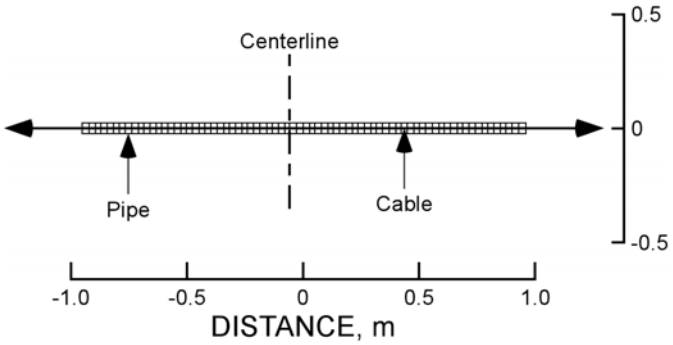

Figure 11.—FLAC model and boundary conditions.

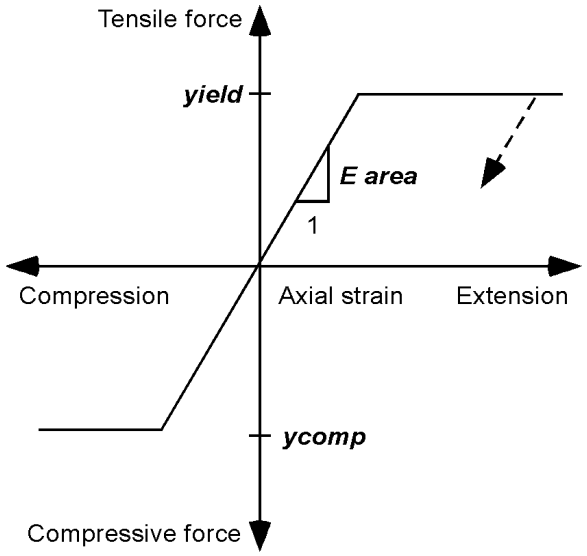

Figure 12.—Axial behavior of FLAC cable element (adapted from Itasca 2000.) Yield = tensile strength, E area = Young's modulus, and ycomp = cross-sectional area.

Table 2.—Cable properties

Property	Model input
Area	1.826 e^{-4} m^2
Young's modulus	128 GPa
Yield	220 kN

The properties that describe grout (see figure 14) are bond stiffness **(kbond)** and shear strength **(sbond)**. Bond stiffness determines the load applied to the cable through the grout as a result of shear displacement between the grout and the cable. It is usually calculated from field pull-out tests, but such data are not available for the current laboratory setup. The FLAC manual provides the following guideline for choosing **kbond** (Itasca 2000).

$$kbond \approx \frac{2\pi G}{10\ln(1+2t/D)} \qquad (3)$$

where G = shear modulus of the grout,

t = radial distance between the cable and the pipe wall,

and D = inside pipe diameter.

For the split-pipe model, a shear modulus of 0.35 w:c grout and a Poisson's ratio of 0.20 are calculated from the upper and lower bounds of Young's modulus of groups using the properties shown in table 3, or 6 e^9 to 8 e^9 N/(m•m).

In previous numerical analyses of pull tests (Ruest 1998), **kbond** was found to be closer to 3.5 e^8 N/(m•m), which is one order of magnitude lower than the value calculated with equation 3. In the current analysis, the importance of **kbond** was assessed by evaluating the cable's response in the range of 1 e^8 to 1 e^{10} N/(m•m).

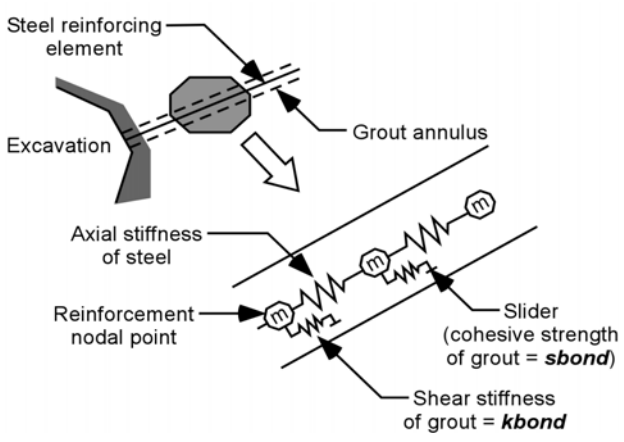

Figure 13.—Illustration of conceptual fully bonded reinforcement (adapted from Itasca 2000).

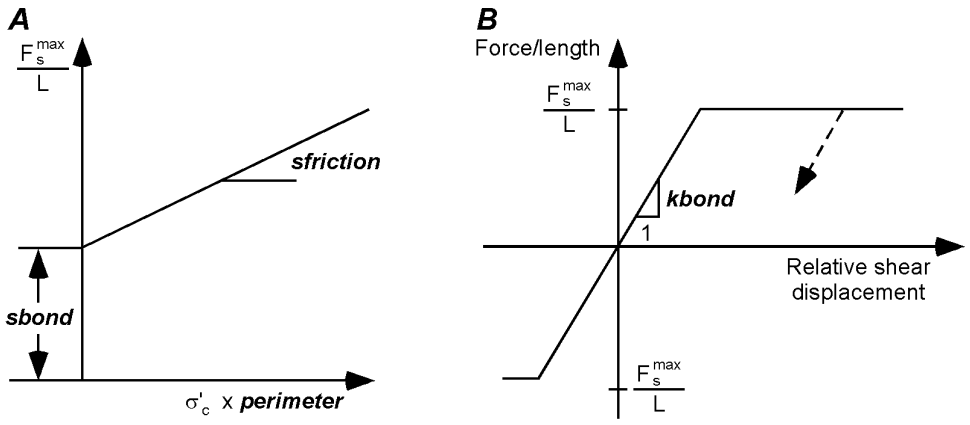

Figure 14.—Grout material behavior for cable elements (adapted from Itasca 2000). *A*, Grout shear strength criterion; *B*, grout shear force versus displacement.

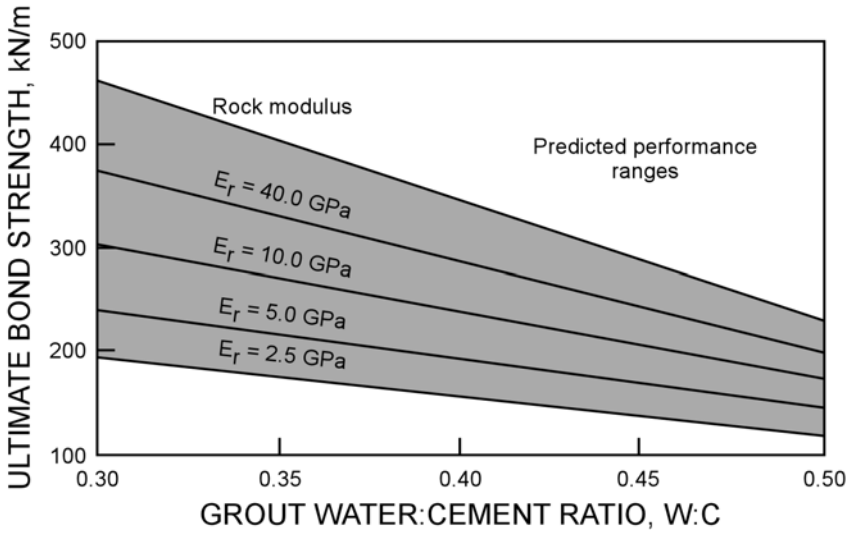

Figure 15.—Ultimate bond strength in kilonewtons per meter as a function of grout quality and rock modulus at 40 mm of slip (Hutchinson and Diederichs 1996). The value of kbond is 1 e^8 to 1 e^{10} N/(m•m), and the value of sbond is 180 to 210 kN/(m•m).

Table 3.—Grout properties

Property	Value
Water:cement ratio	0.35
Poisson's ratio	0.2
kbond (Young's modulus)	6 e^9 - 8 e^9 N/(m•m)

After Hutchinson and Diederichs 1996.

Shear strength determines maximum shear stress in the grout before it begins to slip. Hutchinson and Diederichs (1996) have published values for maximum shear stress (referred to as bond strength) as a function of the Young's modulus of the host rock. An equivalent rock modulus for the experimental pipe assembly is found using the following equation (Hutchinson and Diederichs 1996).

$$\frac{E_r}{(1+\nu_R)d_{BH}} = \frac{2E_p(d_o^{\,2} - d_i^{\,2})}{d_i(1+\nu_p)\{(1-2\nu_p)d_i^{\,2} + d_o^{\,2}\}} \qquad (4)$$

where E_r = rock modulus,

ν_R = rock Poisson's ratio,

d_{BH} = borehole diameter,

E_P = pipe modulus,

ν_P = pipe Poisson's ratio,

d_i = pipe inside diameter,

and d_o = pipe outside diameter.

With the equivalent rock modulus, the value for **sbond** is determined from the plot of rock modulus versus ultimate bond strength (figure 15) (taken as **sbond),** also provided by Hutchinson and Diederichs (1996).

It is well known that increases and decreases in confinement will influence cable bolt behavior. FLAC attempts to account for this effect by relating confinement on the bolt to maximum shear strength. Increases in confinement are followed by increases in the shear strength of the grout according to the strength criterion defined by the parameter **sfriction** and the grouted perimeter **(perimeter)**. In the calibration presented below, no confinement on the cable was modeled (since no confinement was applied to the pipe in the laboratory experiment), and therefore these parameters were irrelevant to the final solution. Thus, only bond stiffness and grout shear strength were varied. The value of **kbond** is 1 e^8 to 1 e^{10} N/(m•m), and the value of **sbond** is 180 to 210 kN/(m•m).

MODEL RESULTS

Once the model was constructed and the boundary conditions applied, the reaction forces at the modeled pipe ends were monitored as the two sides were pulled apart. Once the applied load reached one of the 22-kN increments, load on the cable at 7.6-cm intervals was recorded. The plot in figure 16 shows cable load distribution as calculated by FLAC for an applied load of 22 kN. The plot shows that maximum load is located at the pipe split and that the distribution is symmetrical about the model center. Figure 17 is a plot of shear force at the grout-cable interface. Because the pipe is displaced in both directions, shear forces are negative on the right-hand side of the split and equal but positive on the left-hand side.

Figure 18 is a plot of the averaged laboratory results and the FLAC calculated cable loads for 44- and 117-kN load increments at **kbond** values of 1 e^8, 1 e^9, and 1 e^{10} N/(m•m). The plot indicates that the shape of the FLAC cable curves is very similar to the shape of the idealized laboratory curves for each of the **kbond** values tested, with the lowest stiffness apparently providing the best match with laboratory results. High loads were observed at the split, but decreased with distance from the split. The magnitude of the load at the cable split must be equal to the applied load, but this is not reflected in the plotted data since load is an average across the element.

In each case, the model underpredicts load in the cable at 7.6 cm (near the pipe center). Improvement diminishes with changes in stiffness. The conclusion from this analysis is that, although a reasonable estimate of cable load distribution can be obtained using the previously published equation for **kbond,** a better estimate is obtained using

$$kbond \approx \frac{2\pi G}{100 \ln(1 + 2t / D)} \quad (5)$$

Figure 19 shows a plot of load distributions for the modeled cable at applied loads of 44 and 117 kN for **sbond** values of 180, 190, and 200 kN/m. These values are within the range estimated using Hutchinson and Diederichs' ultimate bond strength plot (figure 10). Only a small amount of variability is apparent in the model results within the range. Note, however, that the ultimate pull-out load will depend on this parameter. For the modeled cable to sustain a load of 178 kN as in the laboratory, a minimum **sbond** of 200 kN/m is required.

FINAL CALIBRATION

Figure 20 is a plot of the FLAC-calculated cable loads compared to laboratory-determined load distributions at applied loads of 44, 89, 133, and 178 kN. The **kbond** and **sbond** values used to obtain these results were l e^8 N/(m•m) and 200 kN/m, respectively, as determined from the parametric analysis above. The plot shows that there is very good agreement between laboratory loads and the loads predicted by FLAC. The load at the split is underpredicted by FLAC, and the difference becomes more significant as load increases. The difference is explained by realizing that the modeled grout remains perfectly intact for the duration of the simulation. In the laboratory tests, the grout deteriorates at the split as the confinement offered by the second pipe is removed. This condition can not be simulated by FLAC. The reader is reminded that the load at the split is necessarily equal to the applied load and that this is not reflected in the data set because no element appears in the model exactly at the split.

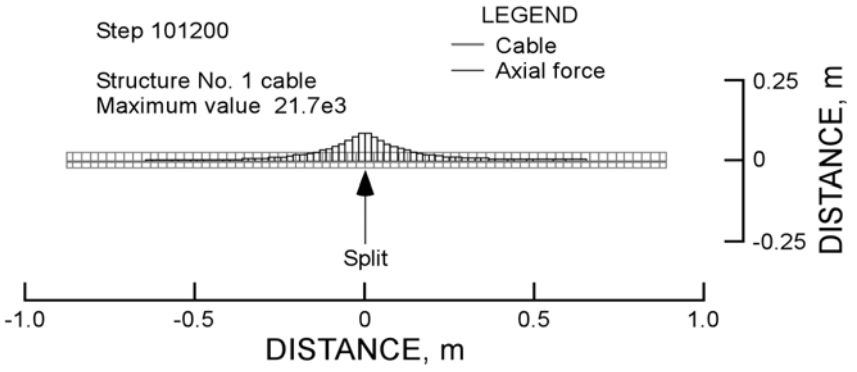

Figure 16.—Plot of load distribution in cable at applied load of 22 kN.

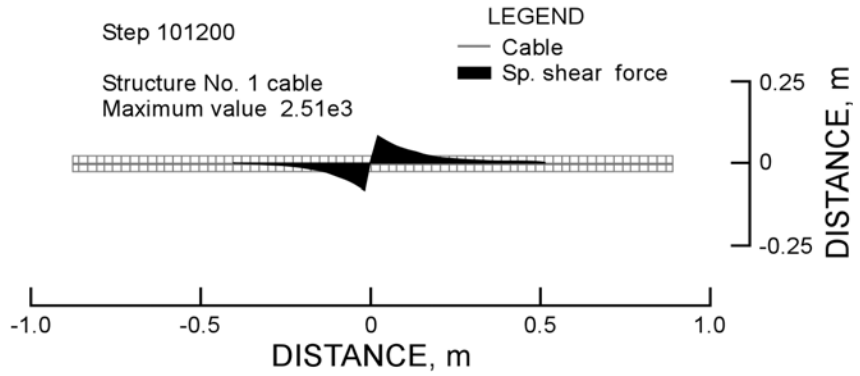

Figure 17.—Plot of shear force at grout-cable interface.

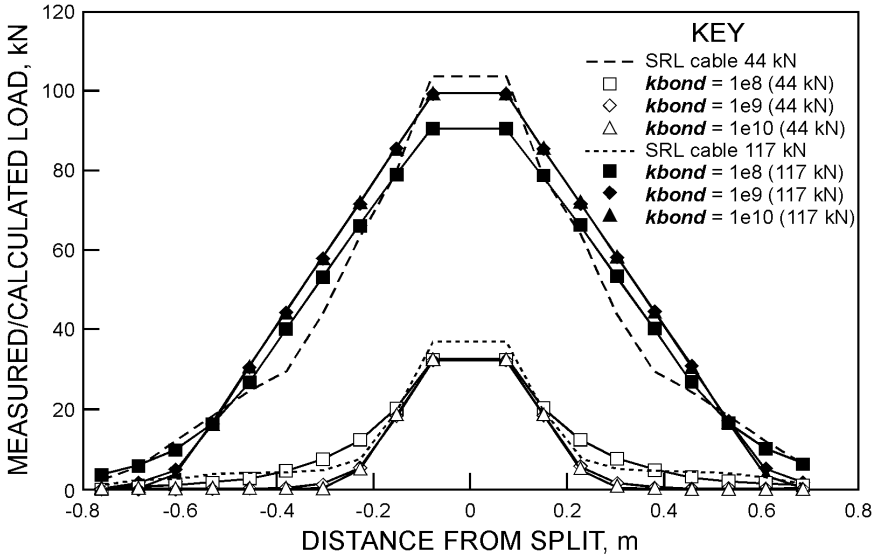

Figure 18.—Load distribution at applied loads of 44 and 117 kN for kbond values of 1 e^8, 1 e^9, and 1 e^{10} N/(m•m).

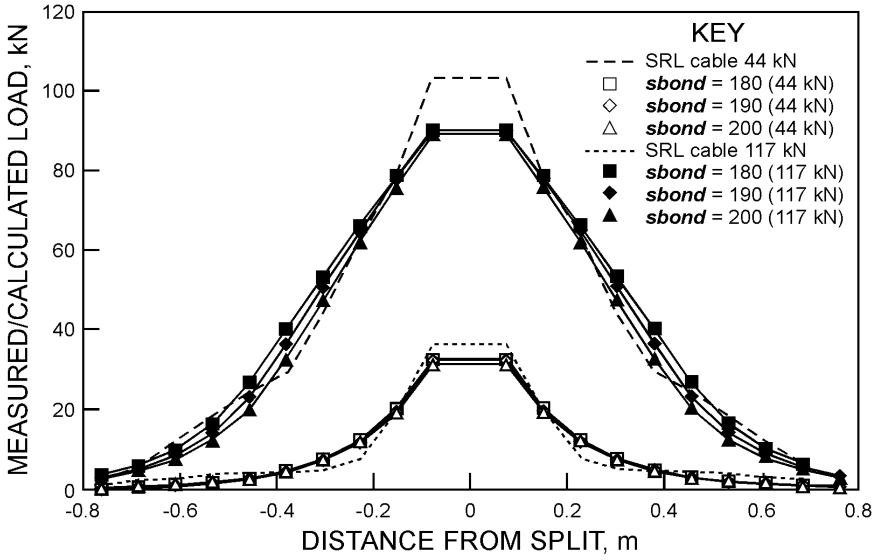

Figure 19.—Load distribution at applied loads of 44 and 117 kN for sbond values of 180, 190, and 200 kN/m.

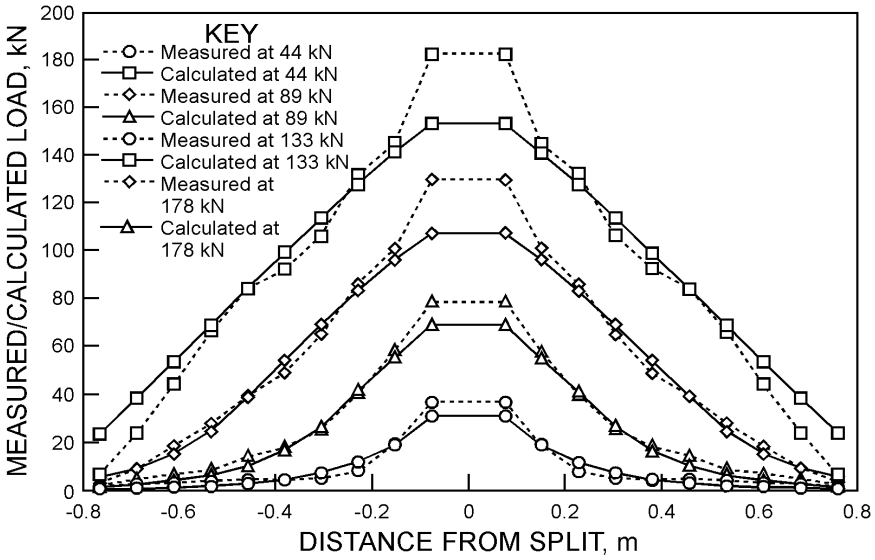

Figure 20.—Plot of laboratory loads and modeled cable loads at 44, 89, 133, and 178 kN.

CONCLUSIONS

CABLE

Pull-test results confirmed that the stiffness of the SRL six-strand cable paralleled that of a standard seven-strand cable, which would ensure that measured strains would also be the strains measured on an adjacent standard cable. The SRL cable can provide a source of reliable point measurements, which can help with evaluations of the effects of cable confinement, grout quality, and rock mass stiffness, among other factors.

The instrumented cable bolt is a unique field and research tool that shows significant potential for improving understanding of the load deformation behavior of grouted cables. Using measured load distribution along a cable will make it possible to (1) predict point loading and load transfer rate along a cable and (2) calculate the stiffness of a grouted cable. The behavior of the SRL six-strand instrumented cable bolt largely parallels the behavior of a standard seven-strand cable in the elastic range; however, this result should be further confirmed in the field.

As mentioned by Windsor (1992), the behavior of a grouted cable bolt needs to be assessed over both short and long intervals. The SRL cable provides insights into how a cable responds to load by measuring loads over short intervals. This tool has the potential to enhance understanding of the overall interaction of cables, rock, and grout.

MODEL

In this investigation, a laboratory split-pipe test on the SRL six-strand instrumented cable bolt was modeled using the continuum code FLAC. Laboratory boundary conditions were reproduced, and modeled cable loads were compared to laboratory-measured cable loads under a variety of grout conditions. Cable properties were kept constant for the calibration, since these are generally well known.

The important conclusion from this analysis is that model parameters can be determined on the basis of engineering principles and published data independent of laboratory results. Although the FLAC cable element is simple, model results indicate very good agreement with the independently determined SRL cable load results. The most significant discrepancy between the two tests was with the 7.6-cm-interval sensor, where modeled cable loads were consistently lower than the laboratory-derived cable loads. The difference between results is either because the grout quality in the model was not reproduced at the split, or because the modeled grout did not reproduce failure and deterioration at the split resulting from cable pull-out. The analysis presented above did not test how FLAC accounts for the effects of confinement, since appropriate data are not available.

It was found that the best agreement between the model and the laboratory experiment was obtained with a grout stiffness **(kbond)** of 1 e^8 N/(m•m) and a maximum shear strength **(sbond)** of 200 kN/m.

REFERENCES

Chekired, M., B. Mokrane, and H.S. Mitri. 1997. CTMD: A New Cable Tension Measuring Device.. Presentation at 99th annual meeting of CIM, Vancouver, BC, April 27-30, 1997, Paper WAM2-El.

Choquet, P., and F. Miller. 1987. Development and Field Testing of a Tension Measuring Gauge for Cable Bolts Used as Ground Support. Presentation at 89th annual meeting of CIM, Toronto, ON, May 3-7, 1987, Paper No. 43, 19 pp.

Goris, J.M. 1990. Laboratory Evaluation of Cable Bolt Supports. U.S. Bureau of Mines Report of Investigations 9308, 23 pp.

Goris, J.M., T.M. Brady, and L.A. Martin. 1993. Field Evaluation of Cable Bolt Supports, Homestake Mine, Lead, SD. U.S. Bureau of Mines Report of Investigations 9474, 28 pp.

Goris, J.M., and J. P. Conway. 1987. Grouted Flexible Tendons and Scaling Investigations. Paper in Improvement of Mine Productivity and Overall Economy by Modern Technology. 13th World Mining Congress (Stockholm, Sweden). Balkema, v. 2, pp. 783-792.

Hutchinson, J.D., and M. Diederichs. 1996. Cablebolting In Underground Mines. Bitech Publishers, Ltd., Richmond, BC. 406 pp.

Hyett, A.J., and W.F. Bawden. 1997. Development of a New Instrumented Cable Bolt to Monitor Ground Support Loads in Underground Excavations. Presentation at 99th annual meeting of CIM, Vancouver, B.C., April 27-30, 1997, Paper WAM2-E3.

Hyett, A.J., M. Moosavi, and W.F. Bawden. 1996. Load Distribution along Fully Grouted Bolts, with Emphasis on Cable Bolt Reinforcement. *International Journal for Numerical and Analytical Methods in Geomechanics*, vol. 20, pp. 517-544.

Itasca Consulting Group, Inc., Minneapolis, MN. 2000. FLAC (Fast Lagrangian Analysis of Continua), Version 4.0.

Milne, D., A. Gendron, and R. Hamilton. 1992. Cable Bolt Research Summary Report. Internal report, Noranda Technology Centre, Montreal, Quebec.

Ruest, M. 1998. Back Analysis of Instrumented Hanging Wall Cable Bolt Reinforcement at Complexe Bousquet. M.Sc. (Eng.) thesis, Queen's University, England.

Windsor, C.R. 1992. Cable Bolting for Underground and Surface Excavations. Paper in Rock Support in Mining and Underground Construction: Proceedings of the International Symposium on Rock Support (Sudbury, ON, June 16-19, 1992). Balkema, pp. 349-376.

Windsor, C.R., and G. Worotnicki. 1986. Monitoring Reinforced Rock Mass Performance. Paper in Proceedings of the International Symposium on Large Rock Caverns (Finland). Pergamon, pp. 1087-1098.